

# Fundamental Key Issues Related to Building Supercritical Carbon Dioxide Brayton Cycle

Won Sup Song

Woodruff School of Mechanical Engineering

Faculty Advisor: Dr. Devesh Ranjan

**Motivation and Objective:** In an effort to reduce environmental pollution and meet future energy demand there is a continuous ongoing search for fossil fuels replacement. Out of these alternative fuel sources, nuclear fuel and concentrated solar power (CSP) promote clean and efficient power conversion for the next generation power plants. The recompression supercritical carbon dioxide (S-CO<sub>2</sub>) Brayton cycle as shown in Figure 1 is theoretically more efficient than the current superheated steam Rankine cycles or the helium Brayton cycle for turbine inlet temperatures > 500°C and is well suited for the nuclear power plants [1]. The S-CO<sub>2</sub> Brayton cycle takes advantage of high fluid density near the critical point to reduce the compression work, thereby, increasing the cycle efficiency. Although the S-CO<sub>2</sub> Brayton cycle is very promising for the CSP applications, significant amount of design challenges needs to be overcome before making this cycle commercially viable for solar applications.

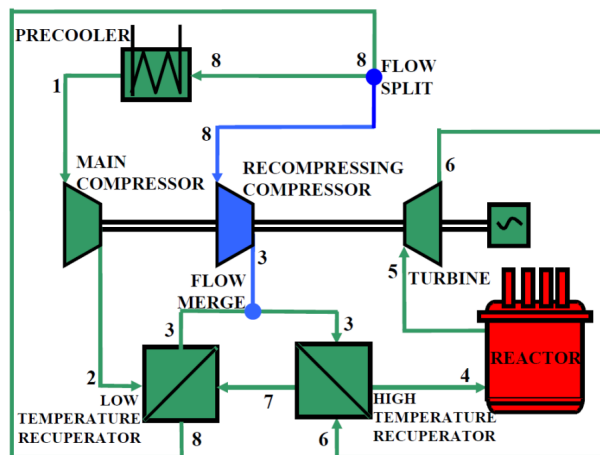


Figure 1: S-CO<sub>2</sub> Brayton Cycle Schematic

## **Research Approach and Scope:**

### Heat Exchanger:

The high fluid density allows a small compressor design, lowering the capital cost. A micro setup can be made to test the heat exchanger efficiency. Heat exchanger efficiency is highly dependent on the fin geometries. Heat exchangers with different fin shapes are shown in Figure 2. Starting from the straight channel, heat exchanger shape has changed over time to produce high heat transfer rate and low pressure drop across the channel. Figure 3 show the Nusselt number, related to heat transfer rate, and fanning friction factor, related to pressure drop of the heat exchangers.

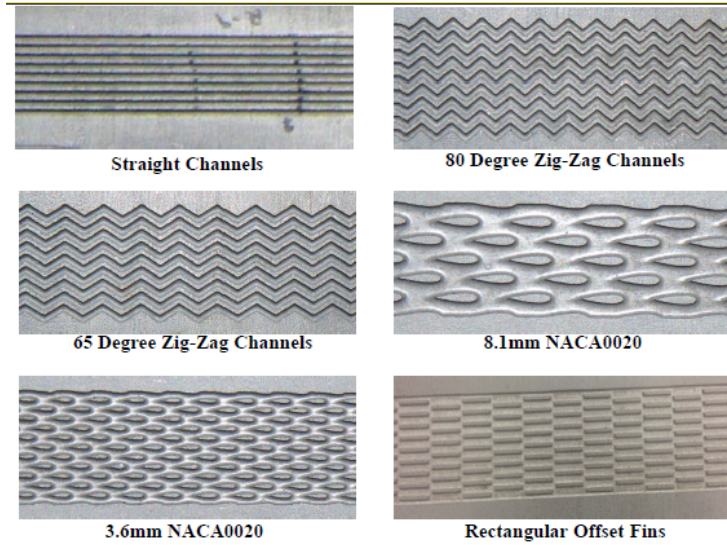


Figure 2: Heat Exchangers with Different Fin Geometries

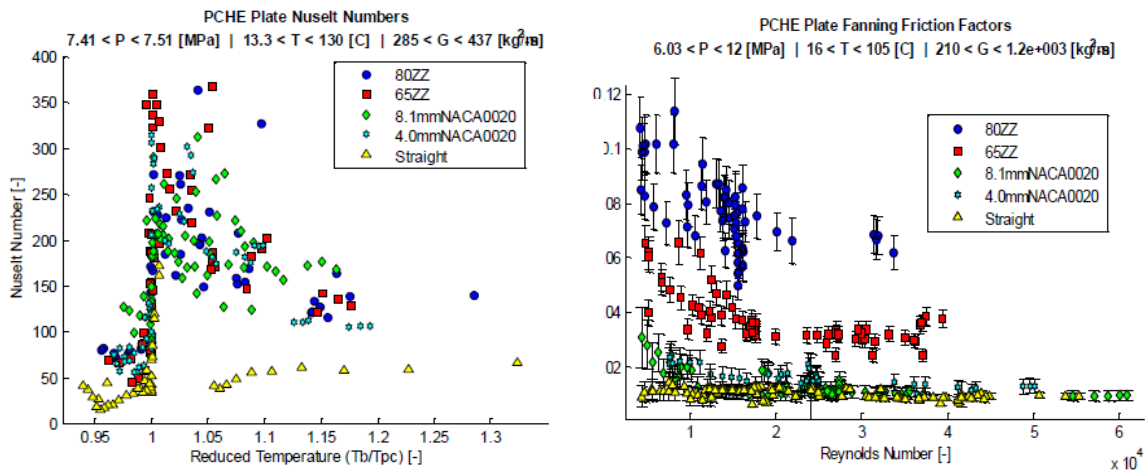


Figure 3: Nusselt Number (Left) and Fanning Friction Factor (right) of Different Heat Exchangers

The zig-zag channel has shown high heat transfer rate, but the continuous zig-zag shape develops boundary layers which causes high pressure drop across the heat exchanger. On the other hand, airfoil channels showed a similar or lower heat transfer rate, but showed lower pressure drop. For our study, the performance of rectangular offset-fin heat exchangers was tested. Due to the vortices formed at the end of each rectangular fins, there is mixing of the fluid which allows higher heat transfer rate. Also, due to the boundary layer dissipation at the end of each fins, the pressure drop is expected to be lower. An experimental setup was made to test these qualities.

### Venturi:

At the inlet of main compressor and at the outlet of turbines, the state is near the boundary that separates the single-phase and two-phase region as shown in Figure 4. The cycle has its maximum efficiency once it operates at high density, single phase flow. Hence, the compressor inlet is exposed to a state near the transition area.

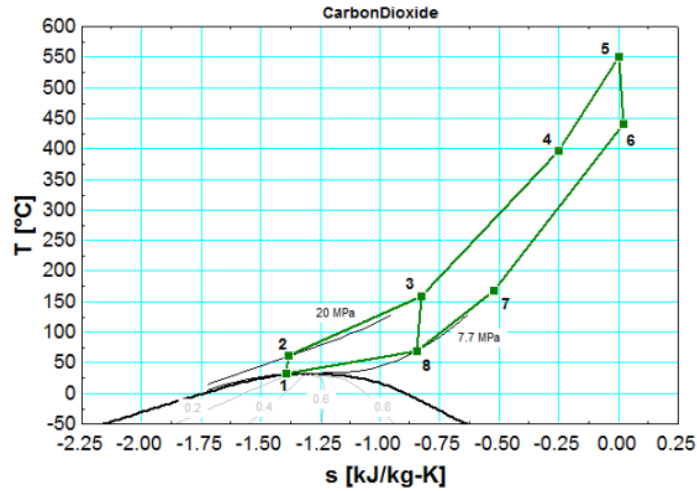


Figure 4: Cycle Schematic of S-CO<sub>2</sub> Brayton Cycle (numbers in figure corresponds to numbers at Figure 1)

The state close to the transition of two-phase region becomes problematic because the local pressure drop occurring at the inlet of compressor shifts the state of flow to the two-phase region as shown in Figure 5. Once it goes to the two-phase region, cavitation, or bubbles form, a process called nucleation. Once cavitation explodes from unstable conditions, it causes damage and corrosion to the turbine blades, which lessens the lifespan of turbines. Our objective is to build a setup that can reproduce the condition occurring at the inlet of compressor and to observe what is happening at the region.

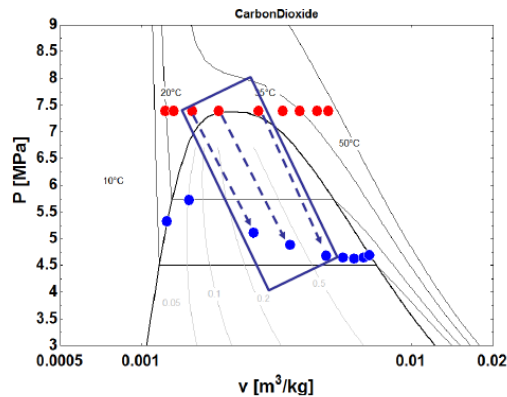


Figure 5: Local Pressure Drop Occurring at the Inlet of Main Compressor

A setup called venturi is made, with an experimental setup schematic as shown in Figure 6. The setup is composed of the test section, shown in Figure 7, that is installed in the cycle to test three characteristics from the experiment:

1. Pressure fluctuation profile when nucleation forms
2. Degree of metal degradation from nucleation
3. Shadowgraphs of nucleation process using optical diagnostic setup

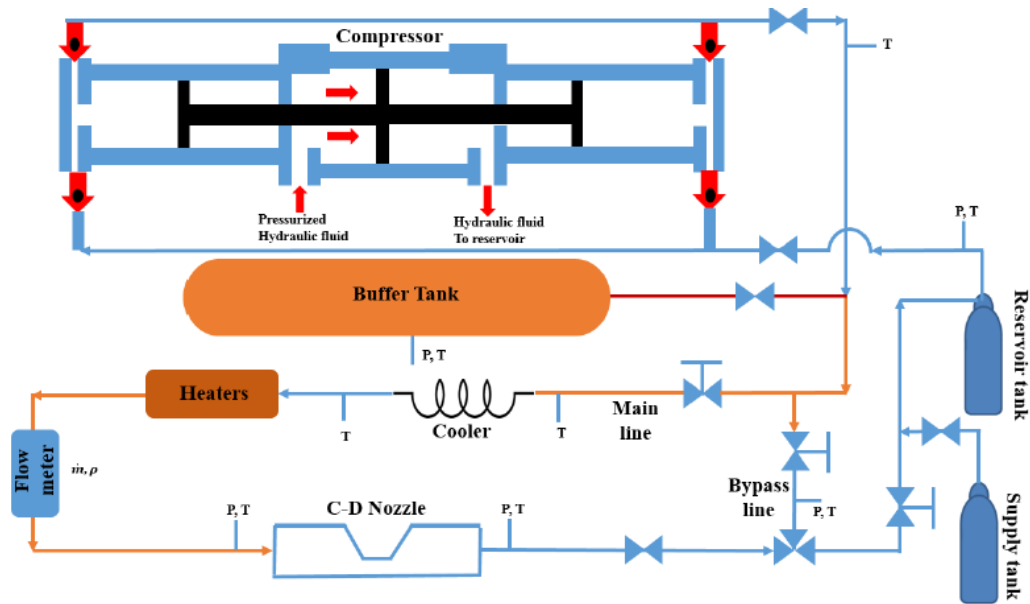


Figure 6: Experimental Setup for Venturi Experiment

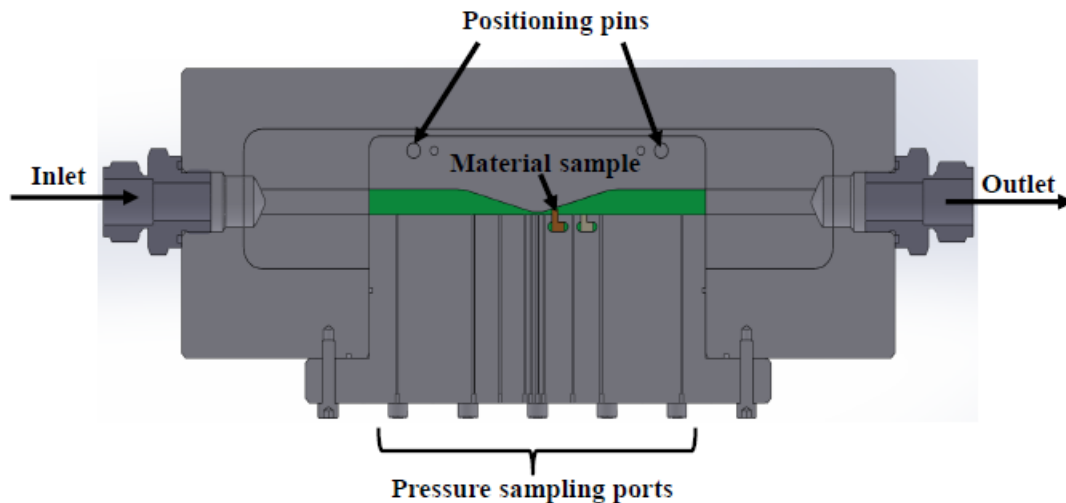


Figure 7: Test Section of Venturi Setup

The test section is made of a converging-diverging system with a condition similar to that of the compressor inlet to produce local pressure drop, which causes nucleation. The pressure fluctuation is measured by placing 10 pressure sensors at 10 different locations of the test section, especially concentrated near the neck where nucleation occurs. A metal piece is placed near the entrance of the diverging system to be allowed degradation. The weight of the metal piece before and after the cycle is run will be measured and will be evaluated to infer how different inlet conditions influence the degree of degradation. Lastly, the nucleation forming will be monitored using a high-speed camera. The process will be displayed as a shadowgraph and optical diagnostic setup will let the camera capture the process of nucleation.

### **Semester Progress and Challenges**

#### **Heat Exchanger:**

The heat exchanger setup was built starting from Fall 2015 semester and continued through this semester. The setup is shown in Figure 8. The cycle is composed of a pressured carbon dioxide tank, buffer tank, heat exchanger, cartridge heater, CO<sub>2</sub> pump, 20 cooling blocks, 20 flowmeters, 60 thermocouples for analyzing heat transfer rate, and two pressure gage sensors for analyzing pressure drop across the test section. The inlet pressure and temperatures are controlled by CO<sub>2</sub> pump (HPLC), shown in Figure 9, and heaters respectively.

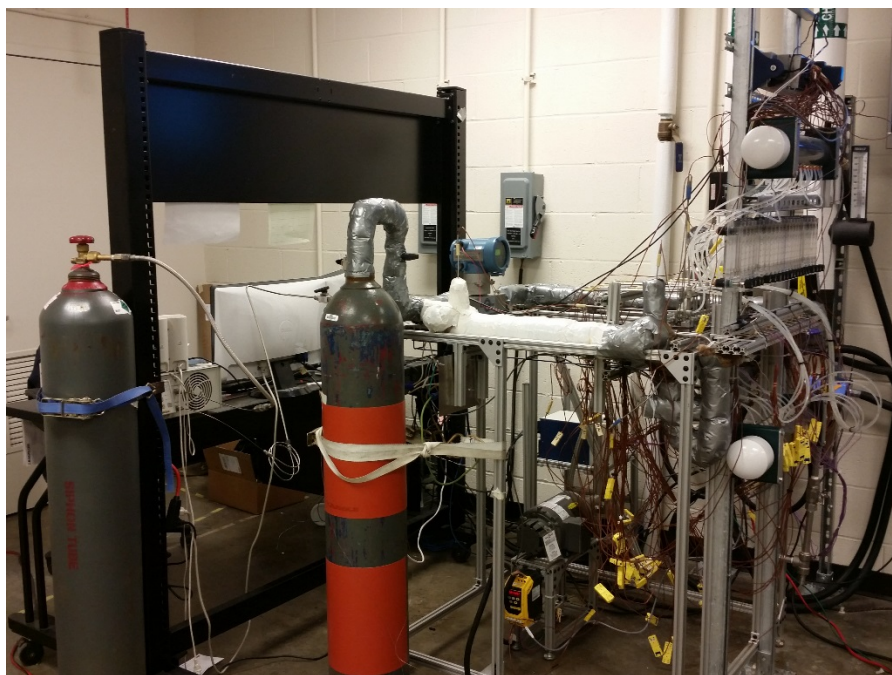


Figure 8: Heat Exchanger Experimental Setup





Figure 9: CO<sub>2</sub> Pump

Installing the heat exchanger required bolting the heat exchanger with a corresponding mating plate along with 20 cooling blocks. The heat exchanger and mating plate are shown in Figure 10. Each bolting torque was minimum 810 lbs-in. and the bolting needed to be done in zigzag pattern across the heat exchanger to ensure homogenized stress distribution. Cooled water, supported by the lab facility, was flown through the channel of cooling blocks and the water volume flow rate was controlled using 20 volume flowmeters as shown in Figure 11. The temperature of the heat exchanger was controlled by the cooled water flowrate. The temperatures of the inlet and outlet of cooled water were measured using 40 thermocouples and temperatures inside the heat exchanger and mating plates were also measured using 20 thermocouples.

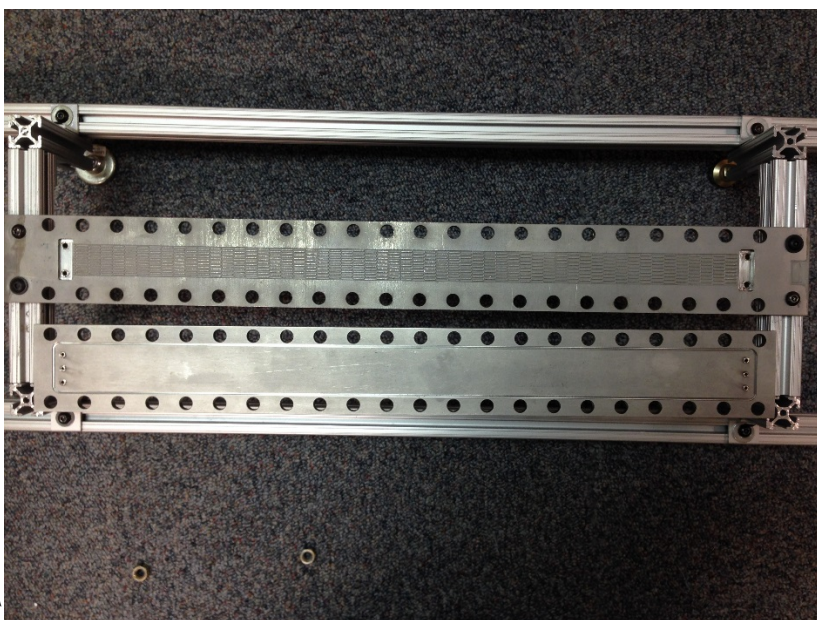


Figure 10: Heat Exchanger (above) and Mating Plate (below)

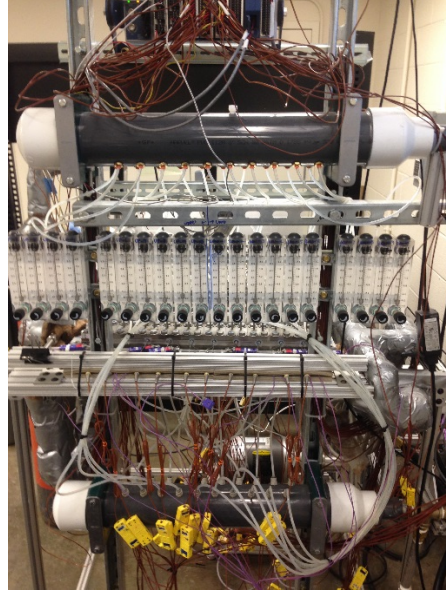


Figure 11: Flowmeter at Heat Exchanger Setup

The temperature read from 60 thermocouples, especially 20 of which are measuring the inside of heat exchanger and mating plate, needs to be accurate to the  $\pm 0.1$  degree Celcius. Heat exchanger thermocouples are inserted through 20 different machined holes half-way through the width of both plates (10 each). The position of the end of the hole needs to be defined with a precise tolerance to predict the degree of linearity of the positions of temperature measurements along the fluid flow. Due to this requirement, factors that influence temperature readings were all analyzed. First, the uneven geometry of the plates affects the measurements, hence, the thickness and width of both heat exchanger and mating plate were measured using a device shown in Figure 12. The measurements were done three times and average values with standard deviation are shown in Figure 13 and 14.

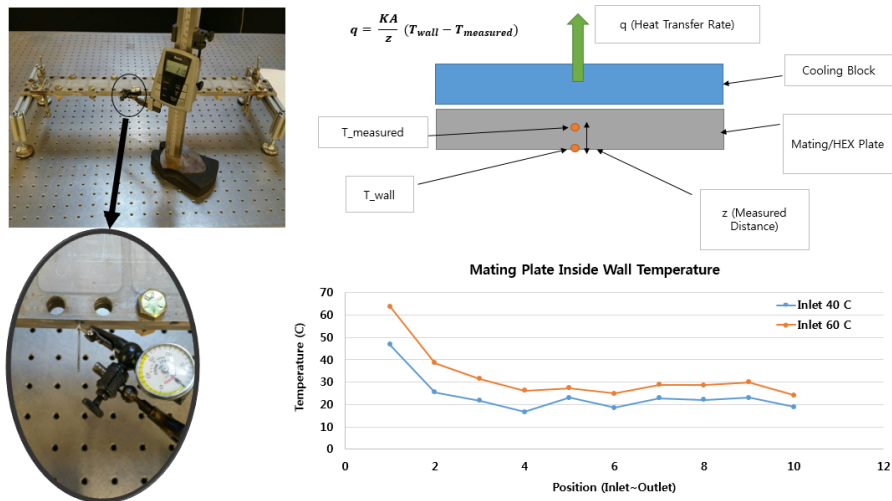


Figure 12: Position Measurement using Tools

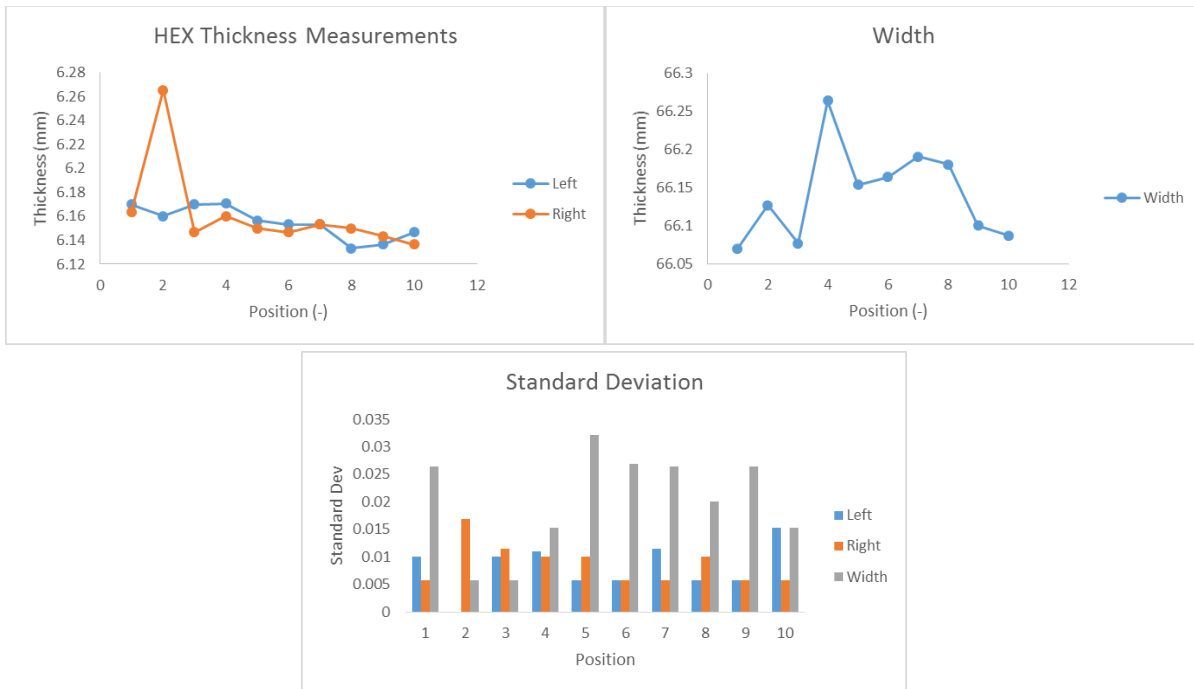


Figure 13: HEX Thickness and Width Measurements

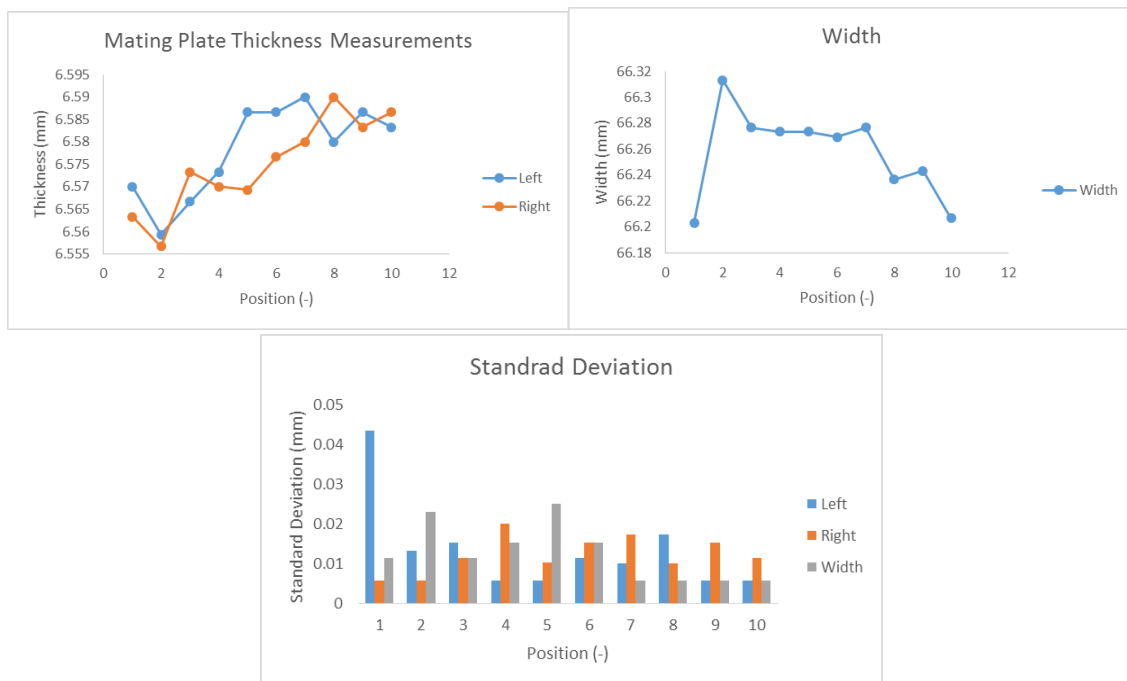


Figure 14: Mating Plate Thickness and Width Measurements



From this result, position of the thermocouples were defined and compared taken into account in calculating heat transfer rate. The result is shown in Figure 15. Based on the analysis, the tolerance was too off such that both heat exchanger and mating plate were not suitable for analysis. EDM companies were contacted to manufacture the plates again with high emphasis on accurate positioning of the hole. Because the diameter of the hole where thermocouples were inserted was very small compared to the depth it went through, only few companies were able to machine it. Based on the tolerance, price, and lead time, we got quotations from 4 companies as well as the GTRI machine shop. Also, the design was changed such that instead of drilling a small hole (1 mm diameter) all the way through the plate, series of drilling with different diameter was requested. In other words, 1.5 mm diameter was drilled half way through the final position, and then 1 mm to the end. This series of drilling ensured higher accuracy in manufacturing. Table 1 shows the companies' quotation and the selected company, which was GTRI due to the accurate tolerance.

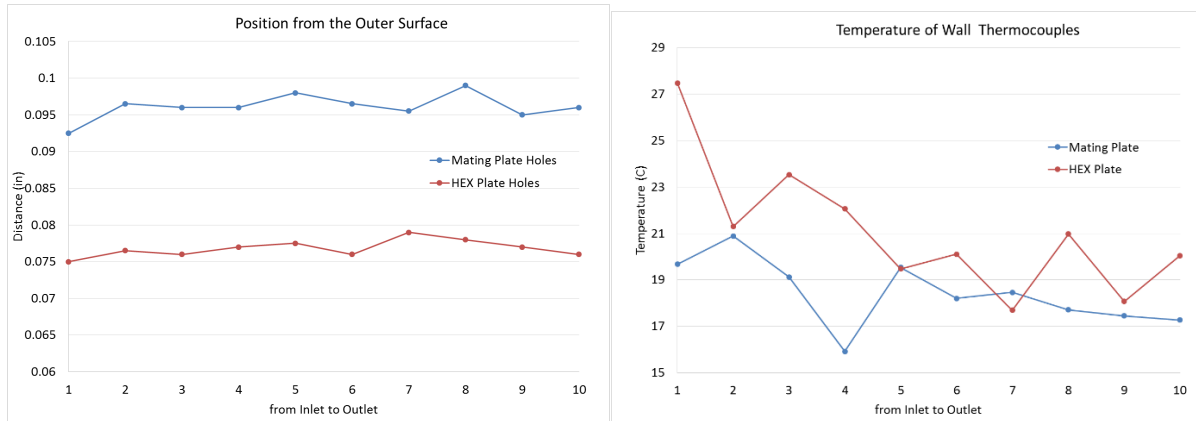


Figure 15: Thermocouple Position and Temperature Measurements

**Table 1. EDM Company Request**

Company	Tolerance	Price	Lead Time	Note
3D Systems	Hole Diameter: +/- 0.04 mm (0.00157") Hole Depth: +/- 0.13 mm (0.00512")	Mating plate: \$300/plate HEX: \$400/plate	14 days/(2 plates)	Several series of drilling was not discussed
WireTech	+/-0.005"	2 HEX Plate & 1 Mating Plates: \$1475 total	Unknown	Recommends drilling holes all the way through 33 mm depth
Smfco	Hole Diameter: +/- 0.005" Hole Depth: +/- 0.010"	Mating Plate: \$570/plate HEX: \$570/plate	Unknown	"
Accu-Tool	Hole Diameter: 0.006" (0.1524 mm) Hole Depth Position: 0.010" (0.254 mm)	\$1500/plate	8 weeks	"
GTRI	0.005"			Selected

After the heat exchanger was manufactured, there was a major problem in finding out the position of the holes. When the hole was drilled with one diameter, a pin of same size could be inserted and could be used to estimate the position of the hidden part. But because the holes were drilled in series, it was impossible for pins to hold its position while measurements were taken place. Therefore, the Panalytical X-ray Facility at Georgia Tech MSE department was contacted to visualize and analyze the hole position, as shown in Figure 16. The angle of the final point with respect to the plate as well as the depth ratio between the half way point and end point were measured using simple image analysis, reading the image in MATLAB and trace each pixels and evaluating from the pixel distances. The results are shown in Figure 17.

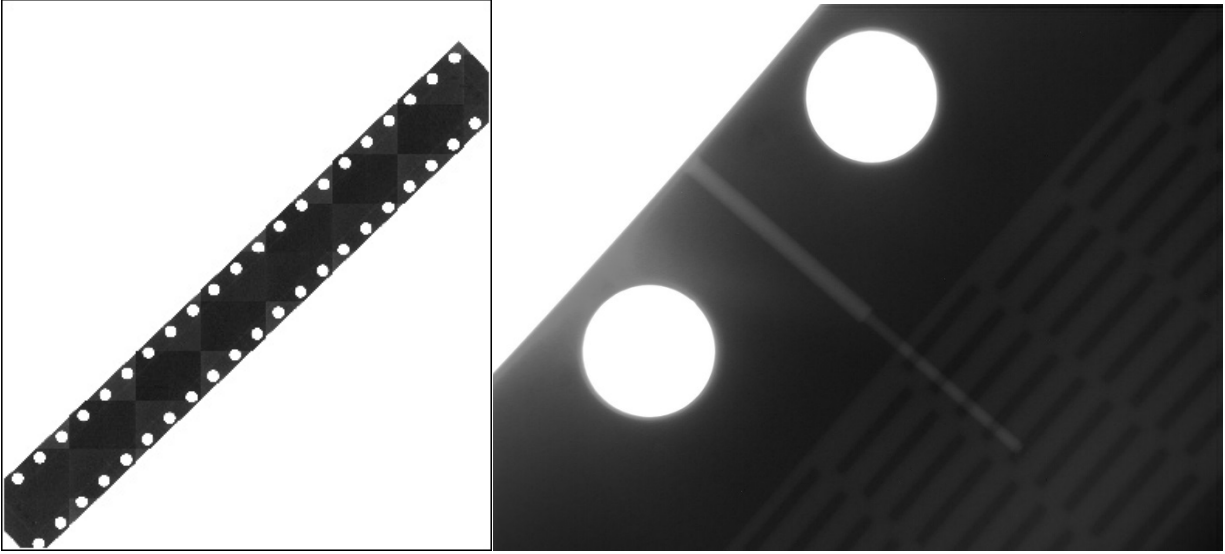


Figure 16: X-ray Inspection of Heat Exchanger and Mating Plate

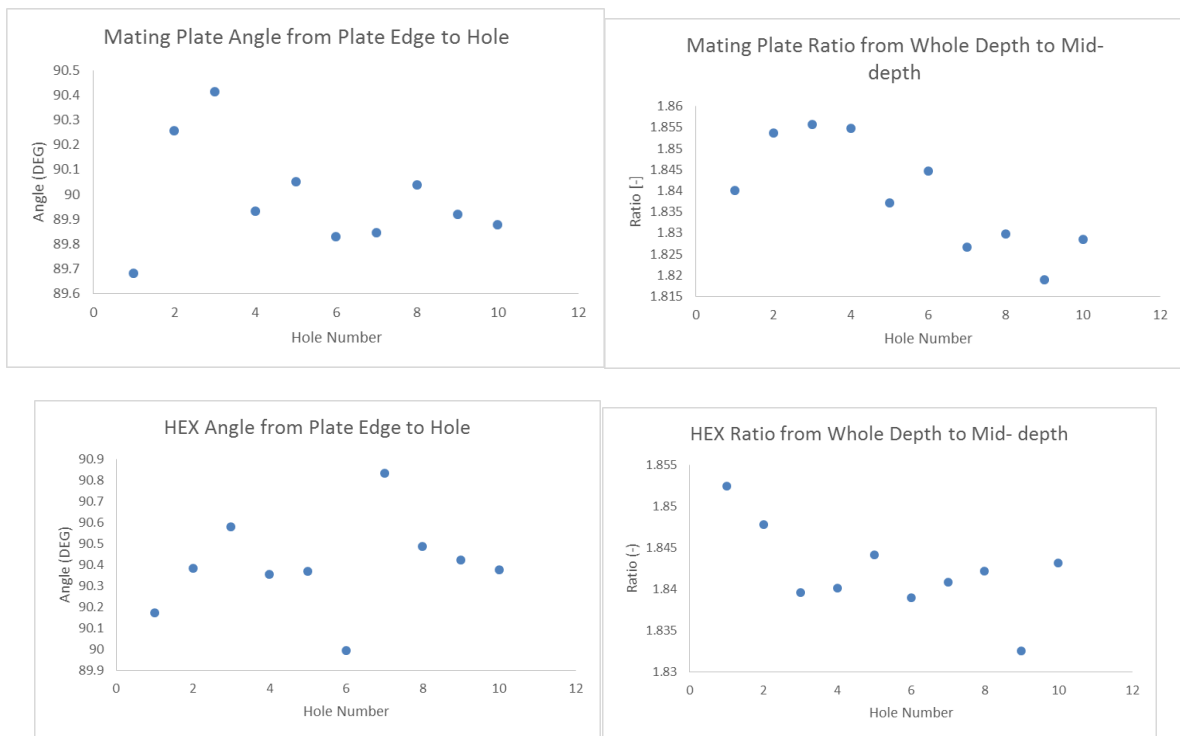


Figure 17: Image Analysis of Mating Plate/HEX X-Ray Pictures (Angle and Depth Ratio)

As the result seems to be promising with little error, the heater/mating plate were evaluated suitable for analysis. For analysis, 60 thermocouples needed to be calibrated with respect to one RTD, which showed accurate readings. However, arranging and organizing 60 thermocouples was difficult and therefore machined holders needed to be made. Because 20 thermocouples were long,

20 were short, and 20 were thin,  $\frac{1}{4}$  inch acrylic sheets were laser-cut to the right dimension so that it can be used for the holders for thermocouples, as shown in Figure 17.

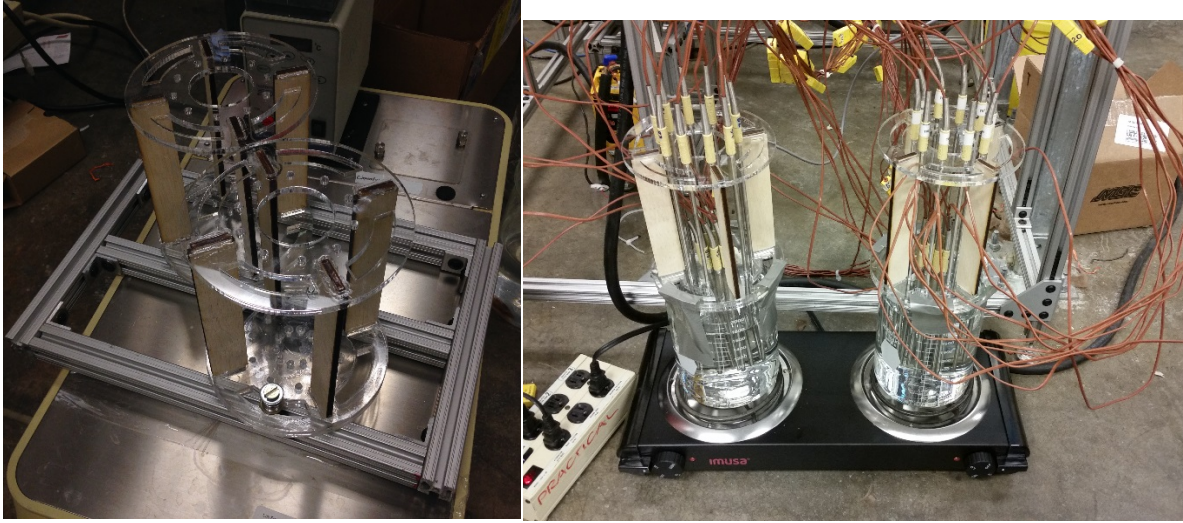


Figure 17: Calibration Tool

After thermocouples were calibrated, the experiment was run and the obtained temperature values were used to calculate the heat transfer rate. It was expected that temperature values decrease along the cooling blocks. As shown in Figures 18 and 19, the heat transfer rate has a steady decrease.

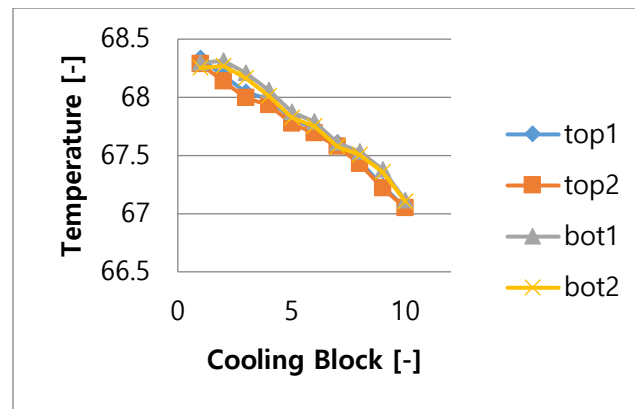


Figure 18: Isothermal State Temperature Changes

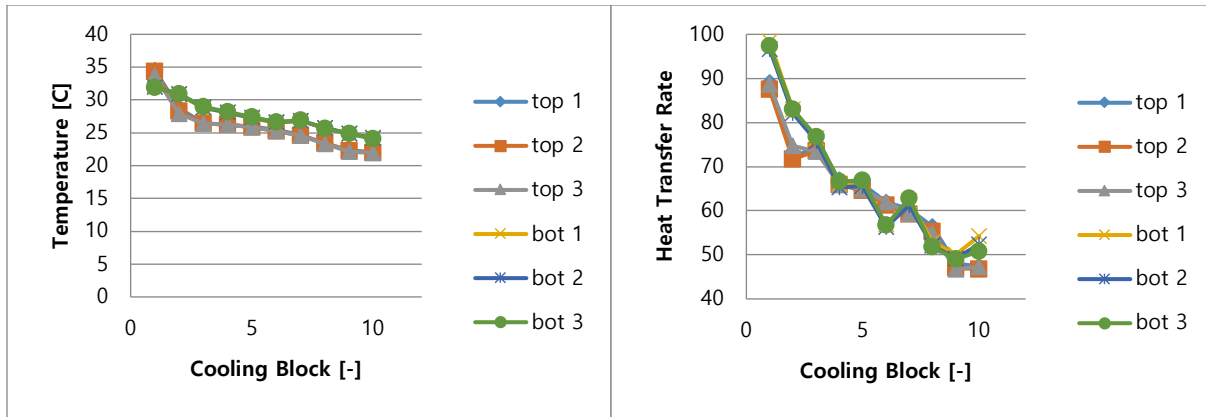


Figure 19: Cooling State Temperature Changes and Heat Transfer Rate

### Venturi:

The venturi setup was built from Fall 2015 semester and continued through this semester. The setup is composed of the test section, compressor, buffer tank, reservoir tank, supply tank, heaters, and flowmeters. Obtaining and connecting all the parts was the main task up until this semester. The test section was manufactured in another department, so majority of time was spent on cutting, bending, and connecting pipes with different diameter sizes, testing leaking of the pipes, testing the compressor, and setting up the optical diagnostic setup. The finished setup was made and is shown in Figure 20. The optical diagnostic setup was set up as in Figure 21. Pressure sensors are installed as in Figure 22. After checking no leaking, when the experiment was run, a primitive shadowgraph image was seen using the camera as shown in Figure 23. In summer and in the future, the shadowgraph image will be more refined and focused so that a detailed nucleation process can be seen. Also, material testing and pressure fluctuation measurements will take place after some more technical problems are solved.



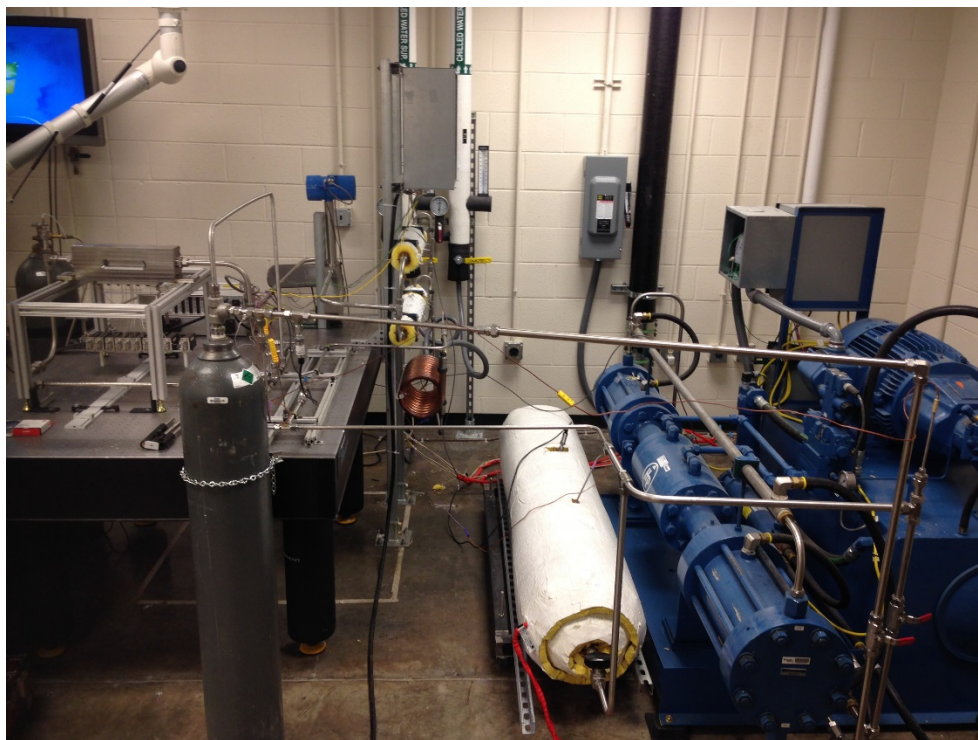


Figure 20: Venturi Experimental Setup

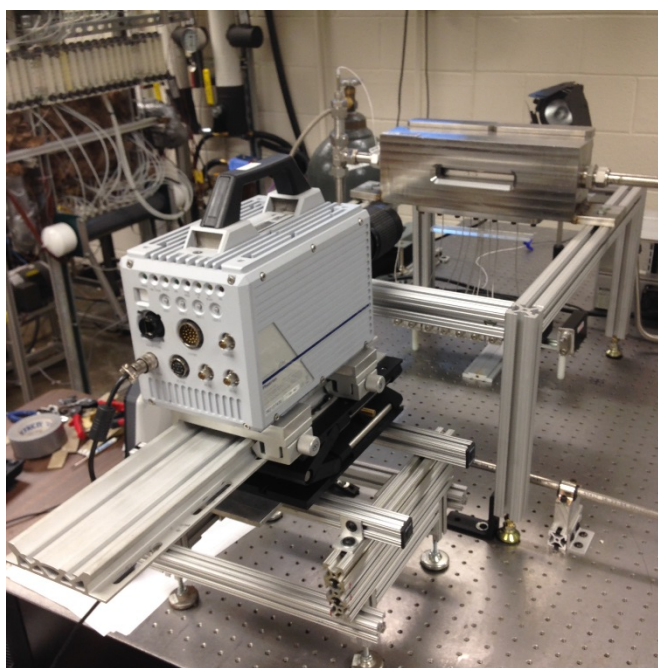


Figure 21: Optical Diagnostics Setup

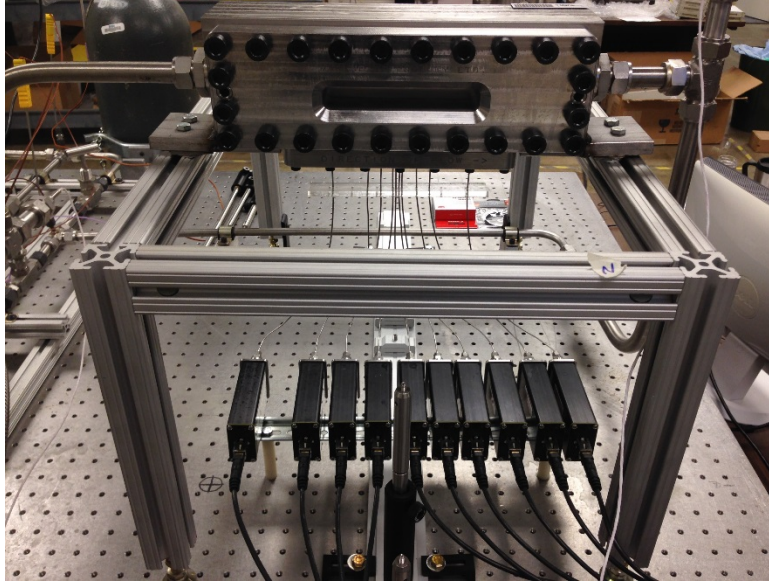


Figure 22: Test Section for Pressure Gages

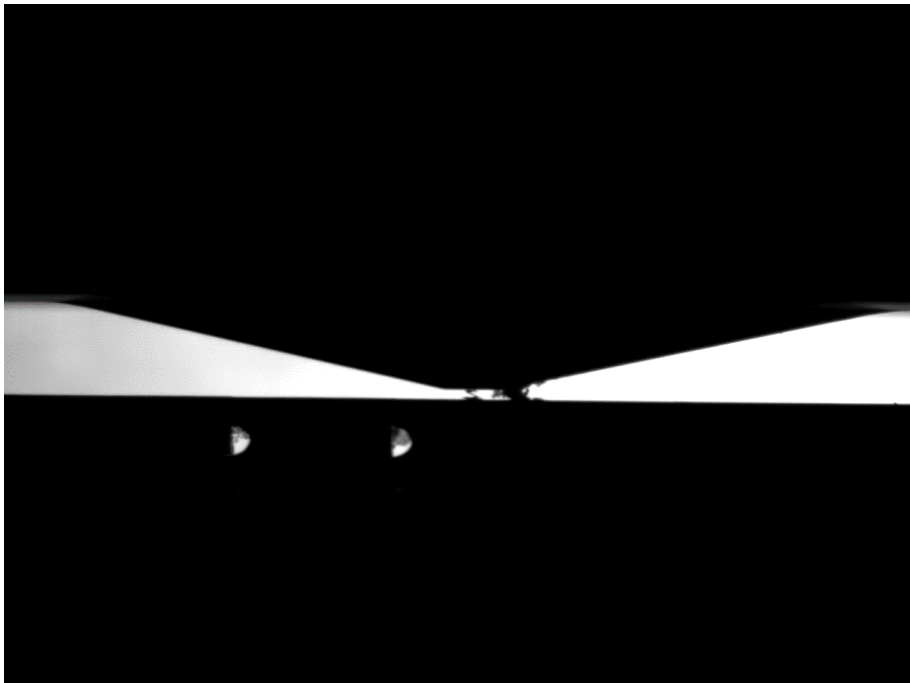


Figure 23: Shadowgraph Image from Veturi Experiment

### **Additional Comments:**

Machining skills as well as piping skills were newly learned so learning was done concurrently as the test sections were built. It was a good opportunity to learn experimental skills and apply learned knowledge in an experimental setup.

### **References**

1. Dostal, Vaclav. "A SUPERCRITICAL CO<sub>2</sub> GAS TURBINE POWER CYCLE FOR NEXT-GENERATION NUCLEAR REACTORS." *ICONE*. Proc. of 10th International Conference on Nuclear Engineering, Arlington, Virginia, Vol. 10. Print. Ser. 22192.